Diarylethene-Powered Light-Induced Folding of Supramolecular Polymers

Takuya Fukushima,[†,∥] Kenta Tamaki,[†,∥] Atsushi Isobe,[†,∥] Takashi Hirose,[¶,⊥] Nobutaka Shimizu,[§] Hideaki Takagi,[§] Rie Haruki,[§] Shin-ichi Adachi,[§] Martin J. Hollamby[¤] and Shiki Yagai*[,‡,#]

[†]Division of Advanced Science and Engineering, Graduate School of Science and Engineering, Chiba University, 1-33 Yayoi-cho, Inage-ku, Chiba 263-8522, Japan

[¶]Institute for Chemical Research, Kyoto University, Uji, Kyoto 611-0011, Japan

[⊥]PRESTO, Japan Science and Technology Agency (JST), 4-1-8 Honcho, Kawaguchi, Saitama 332-0012, Japan

[§]Photon Factory, Institute of Materials Structure Science, High Energy Accelerator Research Organization, Tsukuba 305-0801, Japan

[¤]School of Chemical and Physical Sciences, Keele University, Keele, UK

[‡]Institute for Global Prominent Research (IGPR), Chiba University, 1-33, Yayoi-cho, Inage-ku, Chiba 263-8522, Japan

[#]Department of Applied Chemistry and Biotechnology, Graduate School of Engineering, Chiba University, 1-33 Yayoi-cho, Inage-ku, Chiba 263-8522, Japan

ABSTRACT: Helical folding of randomly coiled linear polymers is an essential organization process not only for biological polypeptides but also for synthetic functional polymers. Realization of this dynamic process in supramolecular polymers (SPs) is however a formidable challenge because of their inherent lability of main chains upon changing an external environment that can drive the folding process (e.g., solvent, concentration and temperature). We herein report a photoinduced reversible folding/unfolding of rosette-based SPs driven by photoisomerization of a diarylethene (DAE). Temperature-controlled supramolecular polymerization of a barbiturate-functionalized DAE (open-isomer) in nonpolar solvent results in the formation of intrinsically curved, but randomly coiled SPs due to the presence of defect. Irradiation of the randomly coiled SPs with UV light causes efficient ring-closure reaction of the DAE moieties, which induces helical folding of the randomly coiled structures into helicoidal ones, as evidenced by atomic force microscopy and small-angle X-ray scattering. The helical folding is driven by internal structure ordering of the SP fiber that repairs the defects and interloop interaction occurring only for the resulting helicoidal structure. In contrast, direct supramolecular polymerization of the ring-closed DAE monomers by temperature control affords linearly extended ribbon-like SPs lacking intrinsic curvature that are thermodynamically less stable compared to the helicoidal SPs. The finding represents an important concept applicable to other SP systems; i.e., post-polymerization (photo)reaction of preorganized kinetic structures can lead to more thermodynamically stable structures that are inaccessible directly through temperature-controlled protocols.

INTRODUCTION

Helical folding of polymers is one of the most important organization processes in biopolymers such as proteins.[1] Through this process, one-dimensional polypeptide chains acquire new physical properties such as stiffness and supramolecular chilarity, which are necessary to construct higher order structures. This beautiful correlation between structures and properties of biopolymers have inspired chemists to develop functional polymers[2–10] or oligomers[11–18] whose chemical design is focused not only on their primary structures but also on their capability to fold into well-defined helical structures. More formidable challenge is to control such folding or also unfolding by external stimuli, particularly through noninvasive one such as light. Hecht and co-workers have applied "backbone approach"[19] by oligomerizing amphiphilic azobenzene units to synthesize rigid foldamer backbones, and successfully controlled the unfolding process of the foldamers as well as revealed its mechanism.[20,21]

Supramolecular polymers (SPs),[22–29] noncovalent polymers that have emerged in the last three decades, have attracted attention because of their properties that are not found in covalent polymers. At first, major attention was focused on their high stimuli-responsiveness due to the reversibility in monomer binding.[30–32] In this decade, however, there is growing interest in the possibility to generate two or more different polymeric assemblies from one monomer by controlling pathway complexity in self-assembly process.[33–46] If the resulting SP chain has capability to change its well-defined conformation in response to light as illustrated by the covalent counterparts, more fruitful outcome of pathway complexity can be envisaged in combination with light stimuli. For SPs, however, the aforementioned backbone approach becomes more challenging because of their inherently dynamic nature in monomer exchange.[36,46] In many cases, photoinduced geometrical change of photoswitches has an impact on the capability of monomers to form main-chain itself, which results in dissociation of SPs.[47–52] Accordingly, it is challenging to design such photoresponsive SPs that are able to fold-up into helical architectures while capable of keeping their main chain structures upon isomerization of embedded photochromic units.

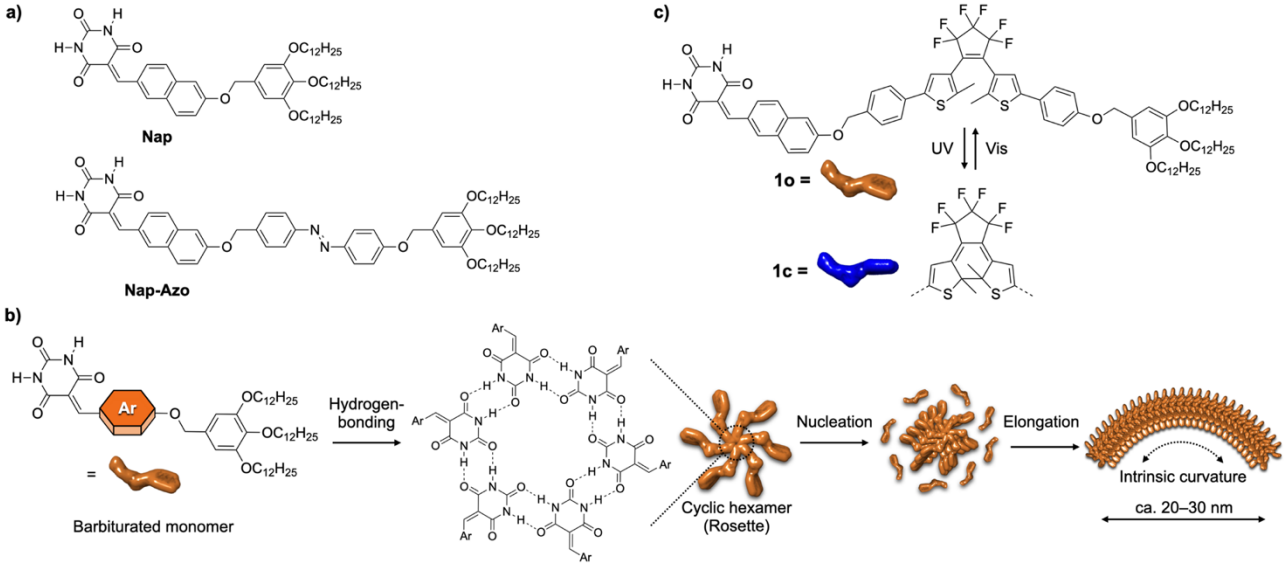

Figure 1. a) Molecular structures of **Nap** (top) and **Nap-Azo** (bottom). b) Supramolecular polymerization process of barbiturated monomers. c) Molecular structure of **1** (**1o** and **1c**).

We recently reported such an exceptional SPs based on a monomer (**Nap-Azo**) composed of barbiturate unit, naphthalene-azobenzene bichromophoric core, and solubilizing aliphatic chains (Figure 1a).[53,54] The barbiturate unit is prerequisite to form a hydrogen-bonded cyclic hexamer, rosette, which undergoes nucleation-elongation type supramolecular polymerization in nonpolar solvents *via* π–π stacking and van der Waals interactions. The 2,6-substituted naphthalene moiety is of secondary importance to impart intrinsic curvature to the resulting SP chains by inducing rotational and translational displacement for rosettes upon stacking (Figure 1b), which has been revealed by using the parent molecule **Nap** (Figure 1a).[55,56] By very slow cooling a hot monomer solution of **Nap-Azo** that allows rosettes to rotate consistently in a uniform direction during supramolecular polymerization, we could obtain helically folded (helicoidal) SPs. Irradiation of the SP solution with UV-light caused partial *trans*-to-*cis* photoisomerization of azobenzene units, which deteriorated the continuous curvature by generating defects and unfolded the helicoidal structures into randomly coiled structures. Although this was the first example of photoinduced "unfolding" of SP fibers, refolding of the randomly coiled structures into the original helicoids could not be realized probably because the resulting structural defect cannot be repaired due to the flexibility of the SP main chain. Indeed, in another paper we found that a monomer with more expanded π-conjugated unit exhibited spontaneous folding of its randomly coiled fibers into helicoidal structures.[57]

Herein we addressed the above unsolved issue, i.e., reversible light-induced folding/unfolding of SPs, by designing diarylethene (DAE)-incorporated barbiturate monomer **1** (Figure 1c). We exploited a DAE's property to modulate π–π stacking tendency through reversible ring-closing/opening photoreactions. DAEs[58,59] have been used to control structures and properties of supramolecular assemblies because of their photoreversible changes in conformational flexibility and extension/reduction of π-conjugation.[60–69] However, most of the reported systems cause photoinduced morphological changes *via* monomer exchange. In the present study, as we will show, UV-induced ring-closure reaction of DAE moieties modulate intrinsic curvature of randomly coiled SPs prepared from the ring-opened DAE monomer **1o**, leading to helicoidal structures composed of the ring-closed DAE monomer **1c**. The photoinduced modulation of the curvature without monomer exchange is suggested by a direct supramolecular polymerization of monomeric **1c**, leading to linearly extended ribbons lacking intrinsic curvature. Evaluation of thermodynamic aspects of the distinct SP structures of **1c** reveals that the linear SPs do not correspond to the global minimum in its free energy surface,[40,42,43] and thermodynamically more stable helicoidal structure can be obtained only through the photoreaction of DAE moieties embedded in the SPs (Scheme 1).

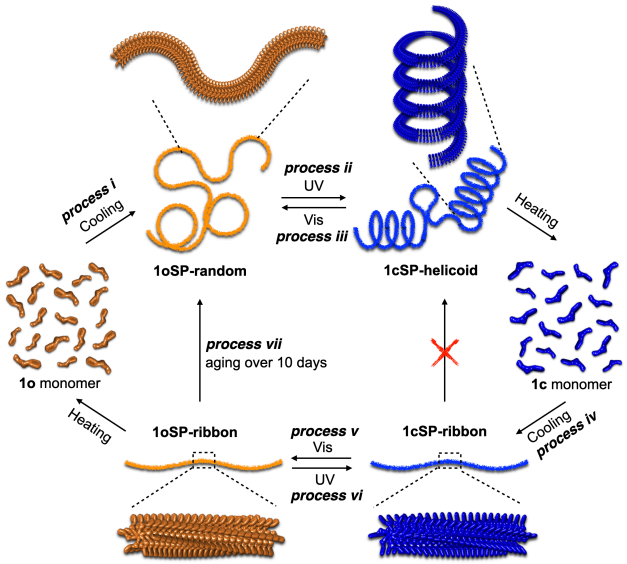

Scheme 1. Schematic representation of pathway dependence in photoresponsive SPs of **1**.

RESULTS AND DISCUSSION

Supramolecular polymerization of 1o (*process i* in Scheme 1). Photoswitchable monomer **1** (Figure 1c) was synthesized according to the scheme shown in the Supporting Information (Scheme S1), and ^{1}H NMR and UV–vis spectra showed that the DAE unit is an open form under room light (**1o**). We prepared SPs of **1o** (c_t = 50 μM) by a temperature-controlled protocol, i.e., cooling a hot methylcyclohexane (MCH) solution with a cooling rate of 1.0 K min^{-1}. The UV–vis absorption spectrum of **1o** measured at 373 K comprises two major absorption bands, one around 300 nm derived from the ring-opened DAE (DAEo) moiety and the other

around 400 nm derived from the naphthalene moiety (red line in Figure 2a). Upon cooling, a new absorption band appeared in the red-shifted region of the naphthalene absorption band, suggesting its J-type stacking (blue line in Figure 2a). The absorption band of the DAEo moiety nearly unchanged upon cooling, suggesting that DAEo moieties are free from defined aggregation. By monitoring the increase of the J-band (λ = 460 nm) as a function of temperature, a specific temperature (ca. 352 K) at which the J-band started to grow was revealed (Figure 2b). Such an abrupt change is a characteristic behavior of cooperative supramolecular polymerization mechanism consisting of nucleation and elongation processes.[70] Because the subsequent heating showed a remarkable thermal hysteresis as discussed later (Figure S1), we withheld to analyze this cooling curve with nucleation-elongation model.[71]

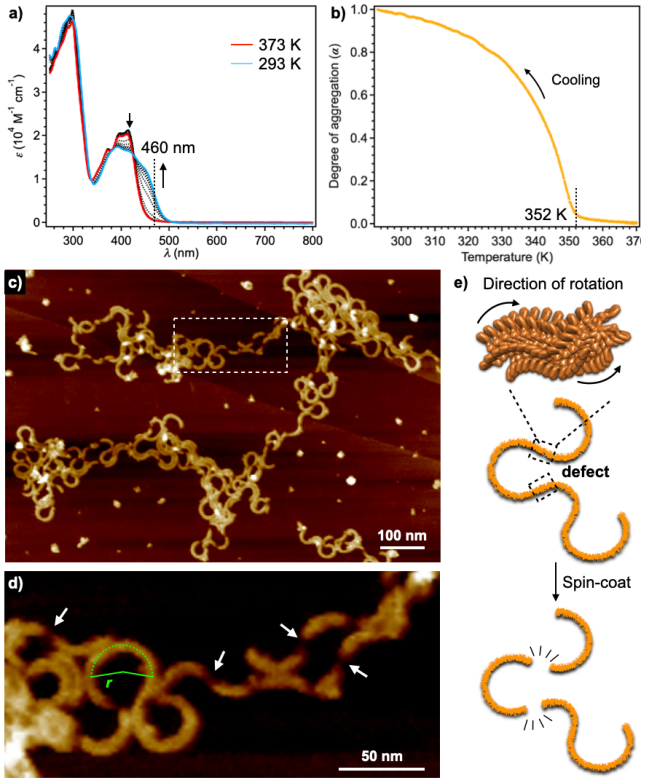

Figure 2. a) Temperature-dependent UV–vis absorption spectra of MCH solution of **1o** (c_t = 50 μM) upon cooling from 373 to 293 K by cooling rate of 1.0 K min^{-1}. Dotted lines show spectra measured at 5 K intervals. b) Plots of degree of aggregation (α, calculated from the absorption change at λ = 460 nm) against temperature. c) AFM image of **1oSP-random** (c_t = 50 μM) spin-coated from the solution onto HOPG substrate. d) Magnification of the dashed square area in c) to highlight the fragmentation of fibers. Green dotted curve indicates an example of manual fitting of curvature to estimate the radius of intrinsic curvature *r*. e) Schematic representation of the fragmentation of **1oSP-random** at defects.

Atomic force microscopy (AFM) images of the above assemblies of **1o**, transferred from the solution onto highly oriented pyrolytic graphite (HOPG) substrate by spin-coating, showed randomly coiled fibers with a uniform curvature (Figure 2c). Hereafter we denote these randomly coiled SPs of **1o** obtained by the cooling protocol as **1oSP-random**. The average radius of curvature (r_{ave}), measured by manually fitting a circle with radius *r* along each curve, was 15.6 ± 0.3 nm (Figures 2d, S2a). This value is almost double of that of the toroidal SPs of the parent molecule **Nap**[56] (r_{ave} = 7.6 ± 0.7 nm), and even larger than that of the randomly coiled SPs of the azobenzene derivative **Nap-Azo**[53] (r_{ave} =10.4 ± 0.2 nm). Accordingly, the DAEo moiety increases r_{ave}. Although most of the **1oSP-random** fibers could be traced about 1 μm in length, they were fragmented in many parts (Figure 2d). The fragmentation was reproducible for the specimens prepared on HOPG substrate by spin-coating or drop-casting, but has been rarely observed when silicon substrate was used for AFM imaging (Figure S3). Because repeated AFM scanning did not cause similar disconnection of fibers, we believe that the fragmentation is caused by tensioning of the SP fibers upon strong adsorption on the HOPG surface in the drying process. It should be noted that the same phenomenon has never been observed for randomly coiled SPs of **Nap-Azo**.[53] Accordingly, the fragmentation is a specific phenomenon occurring for **1oSP-random**, and may reflect their mechanical fragility due to bulky and nonplanar structure of DAEo.

We noticed that the above fragmentation occurs exclusively at the points wherein a turning direction of the curvature changes to the opposite direction, namely, the sigmoidal centers of the two continuous curves (Figure 2d). In our understanding, the change of turning direction of the curvature corresponds to the change the rotational direction of rosettes, and this "defect" differentiate helicoidal and randomly coiled motifs (Figure 2e). Accordingly, the resulting **1oSP-random** fibers are fragmented at the defects probably due to mechanical weakness. In other words, we succeeded in visualizing defects by using AFM.[72–74]

In our previous observations, under kinetic conditions such as fast cooling, the rotational direction of the rosettes changes frequently, resulting in randomly coiled structures. On the other hand, under thermodynamic conditions achieved by much slower cooling (e.g., 0.1 K min^{-1}), we would keep the same rotational direction of rosettes to obtain a helicoidal structure.[53] For **1o**, however, cooling of the monomer solution at 0.1 K min^{-1} also afforded randomly coiled SPs (Figure S4). Hence, **1o** is a molecule that is not polymerized continuously in an orderly fashion, probably due to entropic reasons related to its conformational freedom.

Photoinduced helical folding (*process ii* in Scheme 1). When an MCH solution of **1oSP-random** (c_t = 50 μM) was irradiated at 293 K with UV-light at λ = 293 nm, the absorption band of DAEo attenuated with the growth of a new broad absorption band centered at 585 nm, demonstrating the ring closure reaction of DAE moieties (blue line in Figure 3a). We also observed an appearance of small vibronic peaks in the J-band region of naphthalene moieties (red arrows in Figures 3a, S5a). Because a control experiment using a reference DAE compound demonstrated the ring-closed DAE (DAEc) moiety does not absorb in the J-band region (Figure S5b–d), the small vibronic peaks suggest that the ring-closure reaction of the DAE moiety induce some reorganization of rosette–rosette stacking. The increase of the DAEc absorption band ceased after irradiation for 60 min, suggesting that a photostationary state (PSS_{UV}) was achieved. The **1o**/**1c** ratio at PSS_{UV} was determined to be 20:80 by ^{1}H NMR (Figure S6). Because monomeric **1o** in MCH (c_t = 50 μM at 373 K) and in $CDCl_3$ (c_t = 2 mM, at 293 K) was quantitatively converted to **1c** (Figure S6), the incomplete photoreaction in MCH suggests that DAEo moieties in **1oSP-random** partially adopt conformations not suitable for the ring-closure reaction.[58] We infer that such a conformational variation of the monomer structure is related to the aforementioned defects of SPs (Figure 2e). Dynamic light scattering (DLS) measurements showed that the average hydrodynamic diameter (D_h) observed at 955 nm for pure **1oSP-random** decreased to 712 nm at the PSS_{UV}

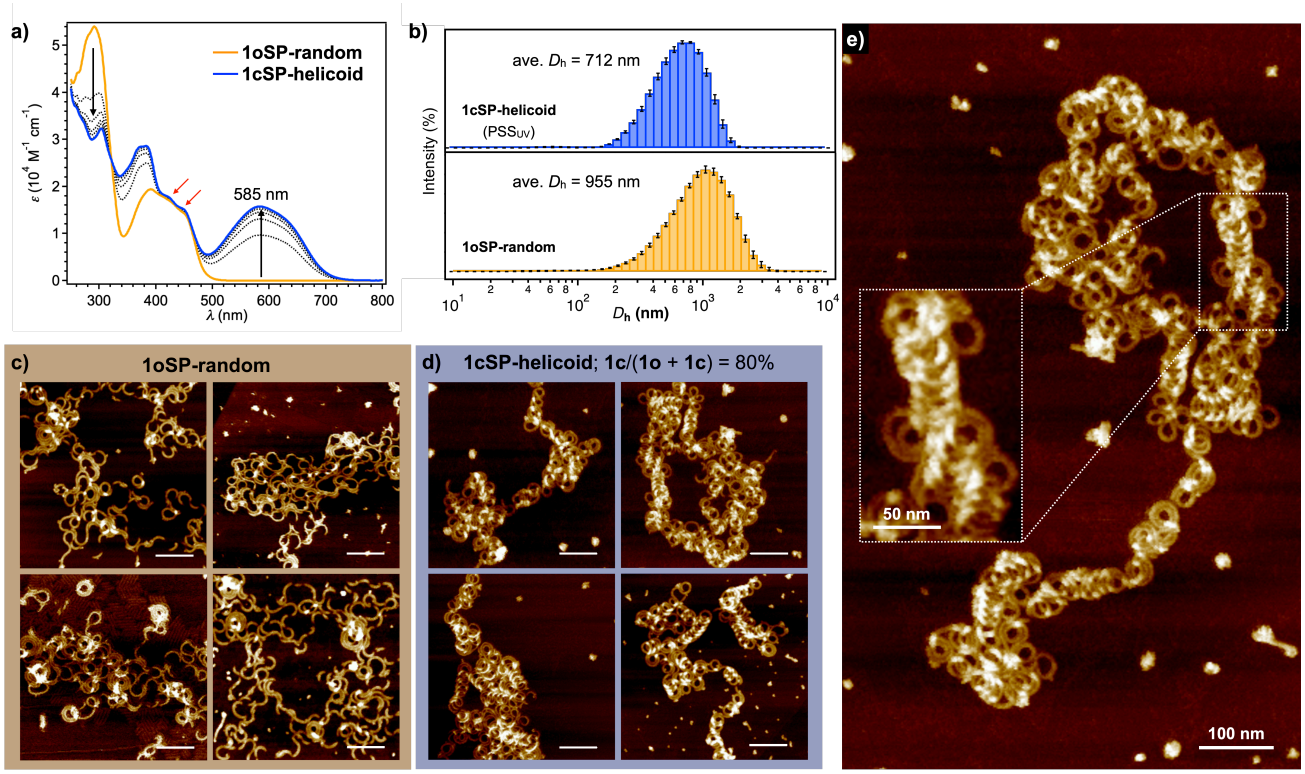

Figure 3. a) UV–vis spectral change from **1oSP-random** to **1cSP-helicoid** upon UV-irradiation for 60 min at 293 K (c_t = 50 μM in MCH). Dotted lines show spectra measured at 10 min intervals. Black arrows indicate the changes upon UV-irradiation. Red arrows indicate small vibronic peaks. b) DLS profiles of the solutions of **1oSP-random** (bottom) and **1cSP-helicoid** (top). Error bas were produced based on four measurements. c,d) AFM images of randomly selected 4 islands of c) **1oSP-random** and d) **1cSP-helicoid** spin-coated from the solutions onto HOPG substrate. Scale bars: 100 nm. e) Magnified AFM image of **1cSP-helicoid**.

(Figure 3b). This suggested that certain change occurred in the SP topology upon the ring-closure reaction of the DAE moieties.

AFM imaging of the above UV-irradiated assemblies, transferred from the solution onto HOPG substrate by spin-coating (c_t = 50 μM in MCH), visualized helicoidal SPs (**1cSP-helicoid**). Figures 3c and 3d display AFM images of randomly selected 4 islands of **1oSP-random** and **1cSP-helicoid**, respectively (magnified 20 images are shown in Figure S7). Approximately six islands of aggregates were found per 1 μm^2 area, and they are well isolated, suggesting that one island corresponds to single SP chain or several SP chains entangled. Compared to divergent morphologies of **1oSP-random** on the substrate, **1cSP-helicoid** are adsorbed on the substrate with more compact morphologies, which is in line with the size decrease in the DLS analysis. Magnified imaging revealed that **1cSP-helicoid** primarily consists of helicoidal domains with persistent length of approximately 100 nm (Figure 3e). The r_{ave} of helicoidal domains was estimated to be 13.6 ± 0.2 nm, which is smaller than r_{ave} of **1oSP-random** (15.6 ± 0.3 nm) (Figure S2b). This result indicates that the intrinsic curvature ($1/r_{ave}$) of supramolecular fibers becomes larger (fibers are more tightly curved) through the ring-closure reaction. The helicoidal structures of **1cSP-helicoid** were preserved in solution over a year as long as the ring-opening reaction of DAE moieties was suppressed in the dark (Figure S8).

Since the reduction of r_{ave} upon the ring-closure reaction apparently corresponds to helical folding of SPs, we further analyzed the folding process by means of *in-situ* small-angle X-ray scattering (SAXS) measurements in MCH. Our previous SAXS studies have shown that our topological SPs exhibit specific X-ray scattering profiles characterized by nonperiodic oscillatory features at Q = 0.3–1.0 nm^{-1}, which arise from the intrinsic curvature of the SPs.[53,56,57,75,76]

Both **1oSP-random** and **1cSP-helicoid** in MCH showed similar nonperiodic oscillatory features at Q = 0.2–1.0 nm^{-1} (orange and blue lines in Figure 4a), and their smallest-Q scattering peaks (peak *n*) were observed at Q = 0.223 nm^{-1} and 0.271 nm^{-1}, respectively, which clearly suggests reduction of r_{ave}. Our previous study revealed that the SAXS profiles of random coil and helicoid could be analyzed using a model representing hollow cylinders.[53,57,75] Data fits (Figure S9) using this model provided r_{ave} values of 16.5 nm for **1oSP-random** and 14.2 nm for **1cSP-helicoid**, respectively, which qualitatively agree well with those estimated from the AFM values (15.6 and 13.6 nm, respectively). Considering the deformation of SPs upon adsorption to HOPG substrate, the larger r_{ave} values in AFM analysis are reasonable.

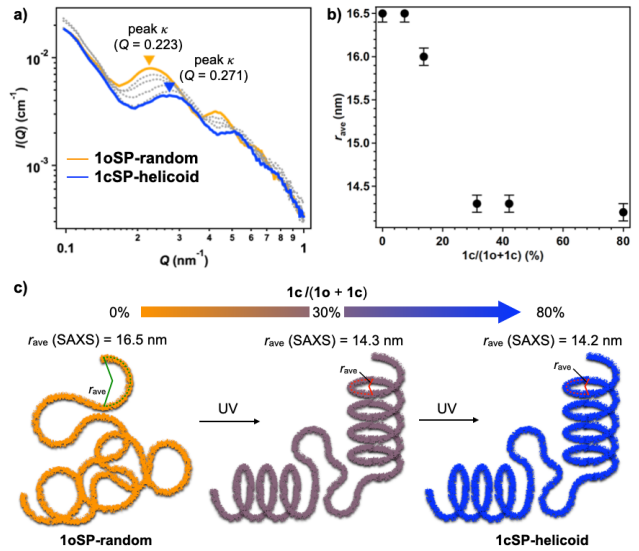

Figure 4. a) Time-dependent SAXS profiles from **1oSP-random** (orange line) to **1cSP-helicoid** (blue line) in MCH upon UV-irradiation for 60 min at 293 K (c_t = 50 μM). Dotted lines show profiles after UV-irradiation for 0.5, 1, 3, and 5 min. b) Plot of SAXS-derived r_{ave} values against **1c**/(**1o** + **1c**) upon UV-irradiation for 60 min. c) Schematic illustration of folding process upon UV-irradiation. The colors of fibers indicate the content of **1c** within SPs.

Figure 4b showed the transition of r_{ave} values of SPs estimated from SAXS analysis as a function of increasing content of **1c** by UV-irradiation. Already at a **1o**/**1c** ratio of 70:30 attained by the initial 5-min UV-irradiation, the transition of the r_{ave} value finished and reached the similar value with that of **1cSP-helicoid** (**1o**/**1c** = 20:80). In line with this observation, an appreciable number of helicoidal structures could be already observed by AFM with the 5-min UV-irradiation (Figure S10). Assuming that the r_{ave} values correspond to the the degree of helical folding, the above result implies that the photogeneration of **1cSP-helicoid** from **1oSP-random** does not originate from a continuous change in the intrinsic curvature, but a phase transition process of supramolecular morphological change, and this phase transition can occur with the ring-closure of about two of six DAE moieties in a rosette (Figure 4c).

The nonlinear emergence of the helicoidal structure with increasing the **1c** fraction strongly suggests that the folding process is a direct process driven by internal structural change of the DAE moieties without monomer exchange. If the photogenerated **1c** in **1oSP-random** forms helicoidal structure by self-sorting and reassembling, the formation of the helicoids should exhibit a more linear response to the fraction of **1c**. Additionally, we confirmed that the direct supramolecular polymerization of **1c** by solvent mixing did not afford helicoidal structure, but form short nanofibers (Figure S11). To the best of our knowledge, the observed single-SP-to-single-SP transition from **1oSP-random** to **1cSP-helicoid** upon UV-irradiation is the first example of the light-induced folding of SPs with retaining the main chain structures. This process is reversibly controlled by a subsequent irradiation with visible light, albeit a very slow dynamics of an unfolding process (*vide infra*).

Photoinduced unfolding (*process iii* in Scheme 1). Unlike the effective folding of **1oSP-random** induced by the ring-closure reaction of DAEo moieties, the opposite process, i.e., unfolding of the resulting **1cSP-helicoid** occurred much slowly in spite of a quick ring-opening reaction of DAEc moieties. When the solution of **1cSP-helicoid** was exposed to visible light (620–645 nm, LED lamp), the absorption band of DAEc isomer quantitatively bleached after 5 min (Figure S12a). In line with this smooth photoreaction, AFM imaging immediately showed randomly coiled structures (Figure 5a), but they contained spiral domains and accordingly a lesser number of mechanically fragile defects was found in comparison to the original **1oSP-random** obtained by cooling (Figure 2c). In accordance with this observation, the radius of curvature (r_{ave}) estimated from the AFM images of this as-photogenerated **1oSP-random** was 14.2 ± 0.2 nm (Figure S12b), which was still much closer to r_{ave} of **1cSP-helicoid** (13.6 ± 0.2 nm), and largely different from r_{ave} of **1oSP-random** (15.6 ± 0.3 nm) obtained by cooling. This was also supported by SAXS analysis, as r_{ave} of the photogenerated **1oSP-random** (14.2 nm) kept almost the same value with that of **1cSP-helicoid** (14.3 nm) at least 3 h from the visible light irradiation (Figure S13a). Hence, the helicoidal domains can be somewhat maintained as spiral domains even after all DAEc moieties are converted to the open-form.

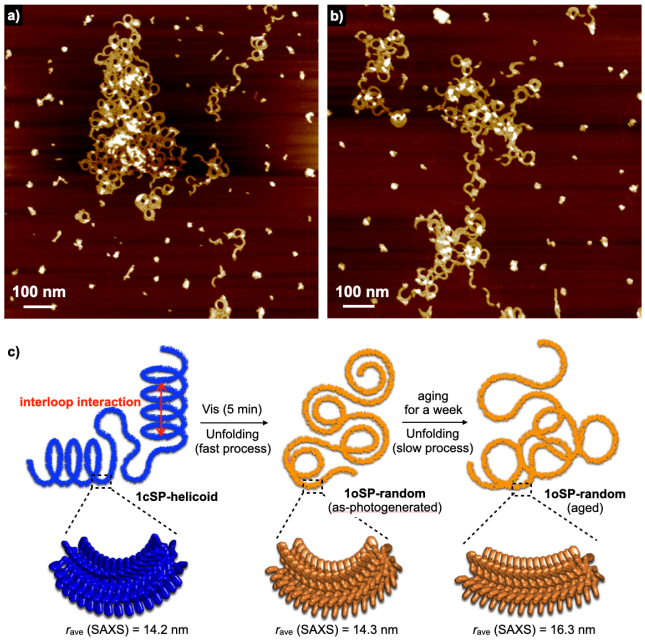

Figure 5. a,b) AFM images of a) as-photogenerated **1oSP-random** and b) additionally 10-days aged **1oSP-random**. c) Schematic representation of unfolding process of **1cSP-helicoid** into **1oSP-random** by visible light irradiation.

The r_{ave} value in SAXS gradually increased over a week, and reached 16.3 nm that is comparable to r_{ave} of the original **1oSP-random** (16.5 nm) prepared by cooling (Figure S13b). AFM imaging after 10-days aging displayed SPs that were unfolded in the similar degree to the original **1oSP-random** with appreciable fragmentation (Figure 5b). When this photogenerated **1oSP-random** was again irradiated with UV-light, we could again see **1cSP-helicoid** by AFM (Figure S12c). These observations suggest unique mechanism underlying the visible light-induced unfolding of **1cSP-helicoid** into **1oSP-random**. The ring-opening of all DAEc moieties in **1cSP-helicoid** does not immediately produce the same degree of defect as the original **1oSP-random**. As discussed later, this hysteretic process is presumably due to the interloop van der Waals interactions of the helicoidal structures (Figure 5c).

Supramolecular polymerization of 1c (*process iv* in Scheme 1). To further study the role of DAEc moieties that can fold-up SP chains by the "post-supramolecular-polymerization photoirradiation", we directly polymerize monomeric **1c** by temperature control. For this purpose, we initially heated the solution

of **1cSP-helicoid** to obtain a monomeric solution of **1c** (containing 20% of **1o**), and then cooled it to 293 K by 1.0 K min^{-1} (Figure S14a,b). To our surprise, the SAXS measurement of thus-prepared SPs of **1c** showed a featureless scattering (purple line in Figure 6a), which could be fitted with a solid cylinder model (radius = 2.34 nm, length ~100 nm). In line with this result, AFM showed only linearly extended ribbons (**1cSP-ribbon**, Figure 6b). Despite the concentration of coexisting **1o** ([**1o**] = 10 μM) is enough to form **1oSP-random** in its pure state (Figure S15), no such randomly coiled structures could be found. This suggests that the coexisting **1o** was not self-sorted, and involved in **1cSP-ribbon**. We also confirmed that the same linear morphology could be obtained from pure **1c** (100%) in a control experiment (Figure S16). The linear morphology was preserved upon aging the solution in the dark over 6 days (Figure S14c,d). Because we have already demonstrated that the *in-situ* photogeneration of DAEc moieties in **1oSP-random** resulted in the formation of **1cSP-helicoid**, the observed linear morphology of **1cSP-ribbon** suggests the presence of supramolecular polymorphism.[77–82] In the absorption spectrum of **1cSP-ribbon**, the J-band of the naphthalene moiety and the visible absorption band of the DAEc moiety are different from that of **1cSP-helicoid** (Figure 6c). We thus infer that the presence of DAEc moieties before polymerization disturbs the specific stacking of rosettes to produce intrinsic curvature probably due to their aggregation.

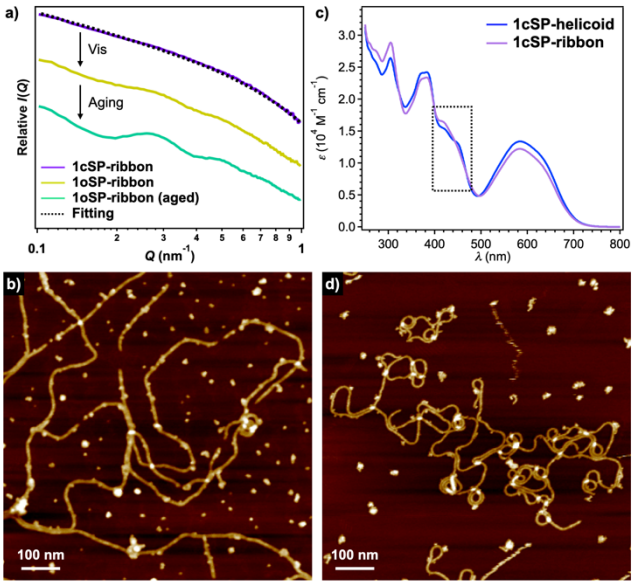

Figure 6. a) SAXS profiles of **1cSP-ribbon** (purple line), **1oSP-ribbon** (yellow line) and 1-week aged **1oSP-ribbon** (green line) in MCH at c_t = 50 μM. The black dashed line is a fit to the data using a solid cylinder model (radius = 2.34 nm, length ~100 nm). b) AFM image of **1cSP-ribbon** (c_t = 50 μM). c) UV–vis absorption spectra of **1cSP-helicoid** (blue line) and **1cSP-ribbon** (purple line) at 293 K. The area surrounded by dotted square is the J-band of the naphthalene moiety. d) AFM image of 1-week aged **1oSP-ribbon** (c_t = 50 μM).

We further investigated whether **1cSP-ribbon** can be converted to **1oSP-random** by visible light (*process v* in Scheme 1). Upon irradiation of **1cSP-ribbon** at 293 K with visible light (620–645 nm, LED lamp), the absorption band of DAEc moiety smoothly attenuated with the recovery of the band of DAEo moiety (Figure S17a). Despite the quantitative ring-opening reaction by 10-min visible-light irradiation, SAXS analysis of the solution did not exhibit any structural features as observed for **1oSP-random** (yellow line in Figure 6a). Furthermore, the absorption band of the naphthalene chromophore of this solution was clearly different from that of **1oSP-random** (Figure S17b). In accordance with these observations, AFM showed linearly extended ribbons (**1oSP-ribbon**, Figure S17c). Upon aging the **1oSP-ribbon** solution for 1 week, some indications of a curved structure became observable by SAXS (green line in Figure 6a) and AFM (Figure 6d). The absorption spectrum also changed to a shape similar to that of **1oSP-random** (Figure S17b). However, the curvature at this stage was still inhomogeneous compared to that of **1oSP-random**, and the fragmentation as observed for **1oSP-random** (Figure 2d) was not observed. These observations accordingly imply that the fragmentation of **1oSP-random** is indeed a specific phenomenon that could occur only at the defects generated in a highly ordered stacking of rosettes leading to intrinsic curvature. Due to the absence of intrinsic curvature, the aged **1oSP-ribbon** was not folded up to **1cSP-helicoid** upon UV-irradiation, and afforded **1cSP-ribbon** with inhomogeneous curvature (*process vi* in Scheme 1). The homogeneously curved structures comparable to **1oSP-random** was observed after prolonged aging for 10 days (Figure S18, process *vii* in Scheme 1).

Mechanism of photoinduced folding. Owing to thermal stability of both isomers of DAE, we were able to estimate thermodynamic parameters of **1oSP-random** and **1cSP-helicoid** by temperature-dependent UV–vis absorption measurements to further understand the photoinduced folding. Upon heating a solution of **1oSP-random** (c_t = 50 μM) at a rate of 1.0 K min^{-1}, the J-band of the naphthalene chromophore (λ = 460 nm) breached with a non-sigmoidal temperature-dependence, suggesting a cooperative mechanism (Figure S19a). As mentioned earlier, the heating curve showed a remarkable thermal hysteresis with respect to the corresponding cooling curve (Figure 2b,S1). We attribute this thermal hysteresis to a kinetic effect in the cooling process, which might be associated with the nucleation of rosettes from various hydrogen-bonded species on the cooling (supramolecular polymerization) process.[83] The solution of **1cSP-helicoid** at the same monomer concentration also showed the similar heating curve (Figure S19c), but it shifted to higher temperature regime compared to **1oSP-random**, suggesting an increase in the thermal stability of **1cSP-helicoid**.

We conducted heating experiments at lower concentrations (10–50 μM) for both the assemblies, and analyzed the resulting heating curves by means of global fitting method using nucleation-elongation model.[84] A modified van't Hoff plot of the natural logarithm of concentrations versus the reciprocal of thus-estimated elongation temperature (T_e) provided standard enthalpy (ΔH°) and entropy (ΔS°) of **1oSP-random** and **1cSP-helicoid** as shown in Table 1 (Figure S19b,d). The ΔH° value of **1oSP-random** (−79.9 kJ mol^{-1}) is larger than that of **Nap** (−72 kJ mol^{-1}), which suggests an additional chromophore in the basic structure of **Nap** increases the aggregation tendency[75,85], enabling **1o** to elongate into open-ended curved SPs. However, due to the conformational flexibility of the monomer, the rosettes cannot continuously stack with a regular conformation and a packing structure, and frequently leave structural defects during polymerization. This process leads to randomly coiled, nonhelical structures (**1oSP-random**). The ring-closure photoreaction of DAEo moieties in **1oSP-random** not only rigidifies the SP main chain but also increases π–π stacking interaction inside the nanofibers, as temperature-dependent UV–vis spectra of **1cSP-helicoid** displayed an appreciable change in the DAEc absorption band upon dissociation (Figure S20).[86] Therefore the reordering of rosette–rosette stacking is believed to occur to some extent, which may repair the structural defects. This internal ordering proceeds throughout the entire fiber without monomer exchange, and eventually folds up a randomly coiled structure into a helicoidal one. The resulting helicoidal structure could be stabilized by the inter-

loop van der Waals interactions between alkyl chains.[57,75] This stabilization may be reflected in a large enthalpic gain ($\Delta(\Delta H^\circ)$ = 40 kJ mol^{-1}) upon the folding of **1oSP-random** into **1cSP-helicoid**. However, the internal ordering through π–π interaction between DAEc moieties might contribute more on the overall stabilization, since our previous study revealed that the stabilization through van der Waals interaction is less than 12 kJ mol^{-1}.[58] On the other hand, the significantly larger ΔS° of **1cSP-helicoid** compared to that of **1oSP-random** ($\Delta(\Delta S^\circ)$ = 111 kJ mol^{-1}) despite structurally more rigid DAEc reflects the interloop interaction that suppresses mobility of alkyl chains.

Table 1. Thermodynamic parameters, ΔH° (kJ mol^{-1}), ΔS° (J mol^{-1} K^{-1}) and ΔG° (kJ mol^{-1}, at 293 K) of four SPs of **1o** and **1c** obtained either by cooling or photoirradiation.

	ΔH°	ΔS°	ΔG° (293 K)
1oSP-random	−79.9	−140	−38.9
↓ UV-light			
1cSP-helicoid	−120	−251	−47.4
↓heating-cooling			
1cSP-ribbon	−82.9	−151	−38.6
↓ visible light			
1oSP-ribbon	−86.9	−181	−39.7

We also recorded temperature-dependent absorption spectra for **1cSP-ribbon** and **1oSP-ribbon** (inhomogeneously curved ribbons) (Figure S19e–h), and evaluated their thermodynamic parameters, which are also shown in Table 1. Comparison of the thermodynamic parameters of linearly extended **1cSP-ribbon** and **1cSP-helicoid** discloses a markedly smaller ΔH° and ΔS° of the former, which further corroborates the presence of the interloop interaction in the latter structure.

The Gibbs free energy changes (ΔG°) of the four SPs at 293 K, estimated from their ΔH° and ΔS° values (Table 1), allowed us to draw the energy landscape of the present system (Figure 7). The appreciable difference between ΔG° of **1cSP-helicoid** and **1cSP-ribbon** ($\Delta(\Delta G^\circ)$ = 8.8 kJ mol^{-1}) with their bistability suggests that the existence of supramolecular polymorphs.[87–89] The thermodynamically more stable **1cSP-helicoid** is not accessible by the direct temperature-activated polymerization of **1c** because the interaction between DAEc moieties disturbs the specific stacking of rosettes to produce intrinsic curvature. In other words, the helical folding requires preorganization of monomers into a randomly coiled structure with curvature by utilizing moderate aggregation tendency of **1o**. Otherwise, **1c** directly organize into linear fibers without curvature due to strong kinetic effect of DAEc moieties in the supramolecular polymerization process. The distinct impact of the DAEc moiety on the folding and supramolecular polymerization processes demonstrates how the selection of right (light) pathway is important to obtain desired supramolecular structures.[90] On the other hand, the comparable ΔG° values of **1oSP-random** and **1oSP-ribbon** ($\Delta(\Delta G^\circ)$ = 0.8 kJ mol^{-1}) is not consistent with the slow conversion of the latter into the former (process *vii* in Scheme 1). Because **1oSP-ribbon** is a kinetic product, it may have been converted to **1oSP-random** during heating.

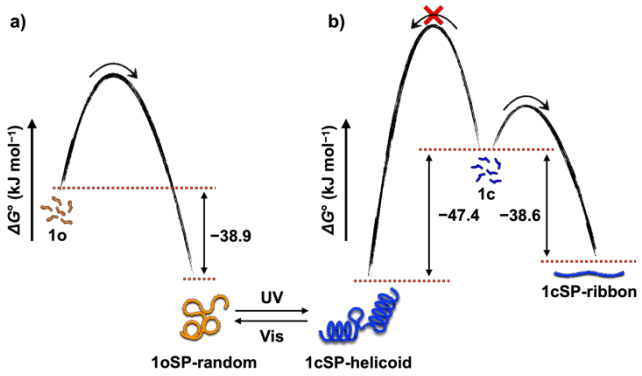

Figure 7. Energy landscape of supramolecular polymerization of a) **1o** and b) **1c**. The thermodynamically stable assembly of **1c** (**1cSP-helicoid**) cannot be accessed by temperature-regulated protocol, but obtained from the preorganized assembly of photoisomer **1o** (**1oSP-random**) through photoisomerization upon UV-irradiation.

CONCLUSIONS

By incorporating the ring-opened isomer of diarylethene into our SP system with intrinsic curvature, we succeeded in helical folding of randomly coiled SPs obtained by a temperature-regulated protocol into the helical structure by light irradiation. This light-induced folding is caused by the ring-closing reaction of the diarylethene moieties, which decreases structural defects associated with the flexible ring-opened diarylethene moieties and increases internal order of the SP backbone, and the resulting helicoidal structures are further stabilized by the interloop van der Waals interactions. Interestingly, when the helicoidal structures of the ring-closed isomer were thermally monomerized, ribbon-like SPs with no curvature were reconstructed by the same temperature-regulated protocol. Thermodynamic analysis demonstrated that the helicoidal structure was thermodynamically more stable than the ribbon-like structure. These results suggest a novel methodology for regulating SPs by a combination of self-assembly and photoisomerization. Namely, photochromic monomers that can aggregate with stronger intermolecular interactions tend to be kinetically trapped upon self-assembly. But if their photoisomers are more weakly interacting to afford preorganized metastable structures, subsequent photoisomerization can lead to thermodynamically stable structures that are different from kinetically trapped ones. This methodology can be applied not only to diarylethenes but also to other photochromic or photoreactive molecules, and hence could expand the scope of supramolecular polymerization.

ASSOCIATED CONTENT

Experimental details, synthetic procedures, compound characterization data, AFM images, spectroscopic data, SAXS analyses (PDF)

Supporting Information

The Supporting Information is available free of charge on the ACS Publications website at DOI: xxxxxxxxxxxxx.

AUTHOR INFORMATION

Corresponding Author

yagai@faculty.chiba-u.jp.

ORCID
Takashi Hirose: 0000-0002-5351-2101
Kenta Tamaki: 0000-0002-2553-8179
Nobutaka Shimizu: 0000-0002-3636-1663

Hideaki Takagi: 0000-0003-3389-7945
Shin-ichi Adachi: 0000-0002-3676-1165
Shiki Yagai: 0000-0002-4786-8603

Author Contributions

‖T. F., K. T., A. I.: These authors contributed equally to this work.

Notes

The authors declare no competing financial interests.

ACKNOWLEDGMENT

This work was also supported by JSPS KAKENHI grant no. 19H02760. S.Y. acknowledges financial support from the Kumagai Foundation for Science and Technology and the Iketani Science and Technology Foundation. This work was performed under the approval of the Photon Factory Program Advisory Committee (Proposal No. 2016G550).

REFERENCES

(1) Englander, S. W.; Mayne, L. The nature of protein folding pathways. *Proc. Natl. Acad. Sci. USA* **2014**, *111*, 15873–15880.
(2) Percec, V.; Ahn, C. -H.; Ungar, G.; Yeardley, D. J. P.; Möller, M.; Sheiko, S. S. Controlling Polymer Shape through the Self-Assembly of Dendritic Side-Groups. *Nature* **1998**, *391*, 161–164.
(3) Yashima, E.; Maeda, K.; Okamoto, Y. Memory of Macromolecular Helicity Assisted by Interaction with Achiral Small Molecules. *Nature* **1999**, *399*, 449–451.
(4) Nakano, T.; Okamoto, Y. Synthetic Helical Polymers: Conformation and Function. *Chem. Rev.* **2001**, *101*, 4013–4038.
(5) Pieroni, O.; Fissi, A.; Angelini, N.; Lenci, F. Photoresponsive Polypeptides. *Acc. Chem. Res.* **2001**, *34*, 9–17.
(6) Yashima, E.; Maeda, K.; Iida, H.; Furusho, Y.; Nagai, K. Helical Polymers: Synthesis, Structures, and Functions. *Chem. Rev.* **2009**, *109*, 6102–6211.
(7) Bléger, D.; Liebig, T.; Thiermann, R.; Maskos, M.; Rabe, J. P.; Hecht, S. Light-Orchestrated Macromolecular 'Accordions': Reversible Photoinduced Shrinking of Rigid-Rod Polymers. *Angew. Chem. Int. Ed.* **2011**, *50*, 12559–12563.
(8) Wang, Y.; Xu, J.; Wang, Y.; Chen, H. Emerging chirality in nanoscience. *Chem. Soc. Rev.* **2013**, *42*, 2930–2962.
(9) Yang, Y.; Zhang, Y.; Wei, Z. Supramolecular Helices: Chirality Transfer from Conjugated Molecules to Structures. *Adv. Mater.* **2013**, *25*, 6039–6049.
(10) Suginome, M.; Yamamoto, T.; Nagata, Y. Poly(quinoxaline-2,3-diyl)s: a fascinating helical macromolecular scaffold for new chiral functions. *J. Synth. Org. Chem. Jpn.* **2015**, *73*, 1141–1155.
(11) Nelson, J. C.; Saven, J. G.; Moore, J. S.; Wolynes, P. G. Solvophobically Driven Folding of Nonbiological Oligomers. *Science* **1997**, *277*, 1793–1796.
(12) Gellman, S. H. Foldamers: a Manifesto. *Acc. Chem. Res.* **1998**, *31*, 173–180.
(13) Berl, V.; Huc, I.; Khoury, R. G.; Krische, M. J.; Lehn, J.-M. Interconversion of single and double helices formed from synthetic molecular strands. *Nature* **2000**, *407*, 720–722.
(14) Hill, D. J.; Mio, M. J.; Prince, R. B.; Hughes, T. S.; Moore, J. S. A field guide to foldamers. *Chem. Rev.* **2001**, *101*, 3893–4011.
(15) Dolain, C.; Maurizot, V.; Huc, I. Protonation-induced transition between two distinct helical conformations of a synthetic oligomer via a linear intermediate. *Angew. Chem. Int. Ed.* **2003**, *42*, 2738–2740.
(16) Khan, A.; Kaiser, C.; Hecht, S. Prototype of a photoswitchable foldamer. *Angew. Chem. Int. Ed.* **2006**, *45*, 1878–1881.
(17) Guichard, G.; Huc, I. Synthetic foldamers. *Chem. Commun.* **2011**, *47*, 5933–5941.
(18) John, E. A.; Massena, C. J.; Berryman, O. B. Helical Anion Foldamers in Solution. *Chem. Rev.* **2020**, *120*, 2759–2782.
(19) Yu, Z.; Hecht, S. Remote control over folding by light. *Chem. Commun.* **2016**, *52*, 6639–6653.
(20) Yu, Z.; Weidner, S.; Risse, T.; Hecht, S. The role of statistics and microenvironment for the photoresponse in multi-switch architectures: The case of photoswitchable oligoazobenzene foldamers. *Chem. Sci.* **2013**, *4*, 4156–4167.
(21) Steinwand, S.; Yu, Z.; Hecht, S.; Wachtveitl, J. Ultrafast Dynamics of Photoisomerization and Subsequent Unfolding of an Oligoazobenzene Foldamer. *J. Am. Chem. Soc.* **2016**, *138*, 12997−1300.
(22) Fouquey, C.; Lehn, J.-M.; Levelut, A.-M. Molecular Recognition Directed Self-Assembly of Supramolecular Liquid Crystalline Polymers from Complementary Chiral Components. *Adv. Mater.* **1990**, *2*, 254–257.
(23) Gulik-Krzywicki, T.; Fouquey, C.; Lehn, J.-M. Electron Microscopic Study of Supramolecular Liquid Crystalline Polymers Formed by Molecular-Recognition-Directed Self-Assembly from Complementary Chiral Components. *Proc. Natl. Acad. Sci. USA* **1993**, *90*, 163–167.
(24) Sijbesma, R.; Beijer, F.; Brunsveld, L.; Folmer, B.J.; Hirschberg, J.; Lange, R.; Lowe, J.; Meijer, E.W. Reversible Polymers Formed from Self-Complementary Monomers Using Quadruple Hydrogen Bonding. *Science* **1997**, *278*, 1601–1604.
(25) Castellano, R. K.; Rudkevich, D. M.; Rebek, J. Polycaps: Reversibly Formed Polymeric Capsules. *Proc. Natl. Acad. Sci. USA* **1997**, *94*, 7132–7137.
(26) Brunsveld, L.; Folmer, B. J. B.; Meijer, E. W.; Sijbesma, R. P. Supramolecular Polymers. *Chem. Rev.* **2001**, *101*, 4071−4097.
(27) Berl, V.; Schmutz, M.; Krische, M. J.; Khoury, R. G.; Lehn, J.-M. Supramolecular Polymers Generated from Heterocomplementary Monomers Linked through Multiple Hydrogen-Bonding Arrays−Formation, Characterization, and Properties. *Chem. Eur. J.* **2002**, *8*, 1227–1244.
(28) De Greef, T. F. A.; Smulders, M. M. J.; Wolffs, M.; Schenning, A. P. H. J.; Sijbesma, R. P.; Meijer, E. W. Supramolecular Polymerization. *Chem. Rev.* **2009**, *109*, 5687–5754.
(29) Aida, T.; Meijer, E. W.; Stupp, S. I. Functional Supramolecular Polymers. *Science* **2012**, *335*, 813–817.
(30) Kim, H.-J.; Lim, Y.-B.; Lee, M. Self-Assembly of Supramolecular Polymers into Tunable Helical Structures. *J. Polym. Sci., Part A: Polym. Chem.* **2008**, *46*, 1925–1935.
(31) Burnworth, M.; Tang, L.; Kumpfer, J. R.; Duncan, A. J.; Beyer, F. L.; Fiore, G. L.; Rowan, S. J.; Weder, C. Optically Healable Supramolecular Polymers. *Nature* **2011**, *472*, 334–337.
(32) Babu, S. S.; Praveen, V. K.; Ajayaghosh, A. Functional π-Gelators and Their Applications. *Chem. Rev.* **2014**, *114*, 1973–2119.
(33) Korevaar, P. A.; George, S. J.; Markvoort, A. J.; Smulders, M. M. J.; Hilbers, P. A. J.; Schenning, A. P. H. J.; De Greef, T. F. A.; Meijer, E. W. Pathway Complexity in Supramolecular Polymerization. *Nature* **2012**, *481*, 492–496.
(34) Ogi, S.; Fukui, T.; Jue, M. L.; Takeuchi, M.; Sugiyasu, K. Kinetic Control over Pathway Complexity in Supramolecular Polymerization through Modulating the Energy Landscape by Rational Molecular Design. *Angew. Chem. Int. Ed.* **2014**, *53*, 14363–14367.
(35) Ogi, S.; Sugiyasu, K.; Manna, S.; Samitsu, S.; Takeuchi, M. Living Supramolecular Polymerization Realized through a Biomimetic Approach. *Nat. Chem.* **2014**, *6*, 188–195.
(36) Albertazzi, L.; Van Der Zwaag, D.; Leenders, C. M. A.; Fitzner, R.; Van Der Hofstad, R. W.; Meijer, E. W. Probing Exchange Pathways in One-Dimensional Aggregates with Super-Resolution Microscopy. *Science* **2014**, *344*, 491–495.
(37) Ogi, S.; Stepanenko, V.; Sugiyasu, K.; Takeuchi, M.; Würthner, F. Mechanism of Self-Assembly Process and Seeded Supramolecular Polymerization of Perylene Bisimide Organogelator. *J. Am. Chem. Soc.* **2015**, *137*, 3300–3307.
(38) Van Der Zwaag, D.; Pieters, P. A.; Korevaar, P. A.; Markvoort, A. J.; Spiering, A. J. H.; De Greef, T. F. A.; Meijer, E. W. Kinetic Analysis as a Tool to Distinguish Pathway Complexity in Molecular Assembly: An Unexpected Outcome of Structures in Competition. *J. Am. Chem. Soc.* **2015**, *137*, 12677–12688.
(39) Rao, K. V.; Miyajima, D.; Nihonyanagi, A.; Aida, T. Thermally Bisignate Supramolecular Polymerization. *Nat. Chem.* **2017**, *9*, 1133–1137.
(40) Sorrenti, A.; Leira-Iglesias, J.; Markvoort, A. J.; de Greef, T. F. A.; Hermans, T. M. Non-equilibrium supramolecular polymerization. *Chem. Soc. Rev.* **2017**, *46*, 5476–5490.
(41) Dhiman, S.; George, S. J. Temporally Controlled Supramolecular Polymerization. *Bull. Chem. Soc. Jpn.* **2018**, *91*, 687–699.
(42) Wehner, M.; Würthner, F. Supramolecular polymerization through kinetic pathway control and living chain growth. *Nat. Rev. Chem.* **2020**, *4*, 38–53.
(43) Ghosh, G.; Ghosh, T.; Fernández, G. Controlled Supramolecular Polymerization of d^8 Metal Complexes through Pathway Complexity and Seeded Growth. *ChemPlusChem* **2020**, *85*, 1022–1033.

(44) Sarkar, S.; Sarkar, A.; George, S. J. Stereoselective Seed-Induced Living Supramolecular Polymerization. *Angew. Chem. Int. Ed.* **2020**, *59*, 19841–19845.
(45) Greciano, E. E.; Calbo, J.; Ortí, E.; Sánchez, L.; N-Annulated Perylene Bisimides to Bias the Differentiation of Metastable Supramolecular Assemblies into J- and H-Aggregates. *Angew. Chem. Int. Ed.* **2020**, *59*, 17517–17524.
(46) Sarkar, A.; Sasmal, R.; Empereurmot, C.; Bochicchio, D.; Kompella, S. V. K.; Sharma, K.; Dhiman, S.; Sundaram, B.; Agasti, S. S.; Pavan, G. M.; George, S. J. Self-Sorted, Random, and Block Supramolecular Copolymers via Sequence Controlled, Multicomponent Self-Assembly. *J. Am. Chem. Soc.* **2020**, *142*, 7606–7617.
(47) Yagai, S.; Karatsu, T.; Kitamura, A. Photocontrollable Self-Assembly. *Chem. Eur. J.* **2005**, *11*, 4054–4063.
(48) Yagai, S.; Kitamura, A. Recent advances in photoresponsive supramolecular self-assemblies. *Chem. Soc. Rev.* **2008**, *37*, 1520–1529.
(49) Yagai, S.; Yamauchi, M.; Kobayashi, A.; Karatsu, T.; Kitamura, A.; Ohba, T.; Kikkawa, Y. Control over Hierarchy Levels in the Self-Assembly of Stackable Nanotoroids. *J. Am. Chem. Soc.* **2012**, *134*, 18205–18208.
(50) Endo, M.; Fukui, T.; Jung, S. H.; Yagai, S.; Takeuchi, M.; Sugiyasu, K. Photoregulated Living Supramolecular Polymerization Established by Combining Energy Landscapes of Photoisomerization and Nucleation − Elongation Processes. *J. Am. Chem. Soc.* **2016**, *138*, 14347–14353.
(51) Fredy, J. W.; Méndez-Ardoy, A.; Kwangmettatam, S.; Bochicchio, D.; Matt, B.; Stuart, M. C. A.; Huskens, J.; Katsonis, N.; Pavan, G. M.; Kudernac, T. Molecular photoswitches mediating the strain-driven disassembly of supramolecular tubules. *Proc. Natl. Acad. Sci. U. S. A.* **2017**, *45*, 11850–11855.
(52) Kartha, K. K.; Allampally, N. K.; Politi, A. T.; Prabhu, D. D.; Ouchi, H.; Albuquerque, R. Q.; Yagai, S.; Fernández, G. Influence of metal coordination and light irradiation on hierarchical self-assembly processes. *Chem. Sci.* **2019**, *10*, 752–760.
(53) Adhikari, B.; Yamada, Y.; Yamauchi, M.; Wakita, K.; Lin, X.; Aratsu, K.; Ohba, T.; Karatsu, T.; Hollamby, M. J.; Shimizu, N.; Takagi, H.; Haruki, R.; Adachi, S.; Yagai, S. Light-induced unfolding and refolding of supramolecular polymer nanofibres. *Nat. Commun.* **2017**, *8*, 15254.
(54) Yagai, S.; Kitamoto, Y.; Datta, S.; Adhikari, B. Supramolecular Polymers Capable of Controlling Their Topology. *Acc. Chem. Res.* **2019**, *52*, 1325–1335.
(55) Yagai, S.; Goto, Y.; Lin, X.; Karatsu, T.; Kitamura, A.; Kazuhara, D.; Yamada, H.; Kikkawa, Y.; Saeki, A.; Seki, S. Self-Organization of Hydrogen-Bonding Naphthalene Chromophores into J-type Nanorings and H-type Nanorods: Impact of Regioisomerism. *Angew. Chem. Int. Ed.* **2012**, *51*, 6643–6647.
(56) Hollamby, M. J.; Aratsu, K.; Pauw, B. R.; Rogers, S. E.; Smith, A. J.; Yamauchi, M.; Lin, X.; Yagai, S. Simultaneous SAXS and SANS Analysis for the Detection of Toroidal Supramolecular Polymers Composed of Noncovalent Supermacrocycles in Solution. *Angew. Chem. Int. Ed.* **2016**, *55*, 9890–9893.
(57) Prabhu, D. D.; Aratsu, K.; Kitamoto, Y.; Ouchi, H.; Ohba, T.; Hollamby, M. J.; Shimizu, N.; Takagi, H.; Haruki, R.; Adachi, S.; Yagai, S. Self-folding of supramolecular polymers into bioinspired topology. *Sci. Adv.* **2018**, *4*, eaat8466.
(58) Irie, M. Diarylethenes for Memories and Switches. *Chem. Rev.* **2000**, *100*, 1685–1716.
(59) Irie, M.; Fukaminato, T.; Matsuda, K.; Kobatake, S. Photochromism of Diarylethene Molecules and Crystals: Memories, Switches, and Actuators. *Chem. Rev.* **2014**, *114*, 12174–12277.
(60) Takeshita, M.; Hayashi, M.; Kadota, S.; Mohammed, K. H.; Yamato, T. Photoreversible supramolecular polymer formation. *Chem. Commun.* **2005**, *6*, 761–763.
(61) De Jong, J. J.D.; Lucas, L. N.; Kellogg, R. M.; van Esch, J. H.; Feringa, B. L. Reversible Optical Transcription of Supramolecular Chirality into Molecular Chirality. *Science* **2004**, *304*, 278–281.
(62) De Jong, J. J. D.; Tiemersma-Wegman, T. D.; van Esch, J. H.; Feringa, B. L. Dynamic Chiral Selection and Amplification Using Photoresponsive Organogelators. *J. Am. Chem. Soc.* **2005**, *127*, 13804–13805.
(63) Katsonis, N.; Minoia, A.; Kudernac, T.; Mutai, T.; Xu, H.; Uji-i, H.; Lazzaroni, R.; De Feyter, S.; Feringa, B. L. Locking of Helicity and Shape Complementarity in Diarylethene Dimers on Graphite. *J. Am. Chem. Soc.* **2008**, *130*, 386–387.
(64) Hirose, T.; Irie, M.; Matsuda, K. Temperature-Light Dual Control of Clouding Behavior of an Oligo(ethylene glycol)-Diarylethene Hybrid System. *Adv. Mater.* **2008**, *20*, 2137–2141.
(65) Yagai, S.; Ishiwatari, K.; Xu, L.; Karatsu, T.; Kitamura, A.; Uemura, S. Rational Design of Photoresponsive Supramolecular Assemblies Based on Diarylethene. *Chem. Eur. J.* **2013**, *19*, 6971–6975.
(66) Yagai, S.; Iwai, K.; Yamauchi, M.; Karatsu, T.; Kitamura, A.; Uemura, S.; Morimoto, M.; Wang, H.; Würthner, F. Photocontrol Over Self-Assembled Nanostructures of π–π Stacked Dyes Supported by the Parallel Conformer of Diarylethene. *Angew. Chem. Int. Ed.* **2014**, *53*, 2602–2606.
(67) Higashiguchi, K.; Taira, G.; Kitai, J.; Hirose, T.; Matsuda, K. Photoinduced Macroscopic Morphological Transformation of an Amphiphilic Diarylethene Assembly: Reversible Dynamic Motion. *J. Am. Chem. Soc.* **2015**, *137*, 2722–2729.
(68) Cai, Y.; Guo, Z.; Chen, J.; Li, W.; Zhong, L.; Gao, Y.; Jiang, L.; Chi, L.; Tian, H.; Zhu, W. Enabling Light Work in Helical Self Assembly for Dynamic Amplification of Chirality with Photoreversibility. *J. Am. Chem. Soc.* **2016**, *138*, 2219–2224.
(69) Adhikari, B.; Suzuki, T.; Xu, L.; Yamauchi, M.; Karatsu, T.; Yagai, S. Photoresponsive supramolecular copolymers from diarylethene-perylene bisimide hydrogen bonded complexes. *Polymer* **2017**, *128*, 356–362.
(70) Smulders, M. M. J.; Nieuwenhuizen, M. M. L.; de Greef, T. F. A.; van der Schoot, P.; Schenning, A. P. H. J.; Meijer, E. W. How to distinguish isodesmic from cooperative supramolecular polymerisation. *Chem.Eur. J.* **2010**, *16*, 362–367.
(71) Zhao, D.; Moore, J. S. Nucleation–elongation: a mechanism for cooperative supramolecular polymerization. *Org. Biomol. Chem.* **2003**, *1*, 3471–3491.
(72) Bochicchio, D.; Salvalaglio, M.; Pavan, G. M. Into the Dynamics of a Supramolecular Polymer at Submolecular Resolution. *Nat. Commun.* **2017**, *8*, 147.
(73) Thota, B. N. S.; Lou, X.; Bochicchio, D.; Paffen, T. F. E.; Lafleur, R. P. M.; van Dongen, J. L. J.; Ehrmann, S.; Haag, R.; Pavan, G. M.; Palmans, A. R. A.; Meijer, E. W. Supramolecular Copolymerization as a Strategy to Control the Stability of Self-Assembled Nanofibers. *Angew. Chem. Int. Ed.* **2018**, *57*, 6843–6847.
(74) Bochicchio, D.; Kwangmettatam, S.; Kudernac, T.; Pavan, G. M. How Defects Control the Out-of-Equilibrium Dissipative Evolution of a Supramolecular Tubule. *ACS Nano* **2019**, *13*, 4322–4334.
(75) Aratsu, K.; Takeya, R.; Pauw, B. R.; Hollamby, M. J.; Kitamoto, Y.; Shimizu, N.; Takagi, H.; Haruki, R.; Adachi, S.; Yagai, S. Supramolecular copolymerization driven by integrative self-sorting of hydrogen-bonded rosettes. *Nat. Commun.* **2020**, *11*, 1623.
(76) Datta, S.; Kato, Y.; Higashiharaguchi, S.; Aratsu, K.; Isobe, A.; Saito, T.; Prabhu, D. D.; Kitamoto, Y.; Hollamby, M. J.; Smith, A. J.; Dagleish, R.; Mahmoudi, N.; Pesce, L.; Perego, C.; Pavan, G. M.; Yagai, S. Self-assembled poly-catenanes from supramolecular toroidal building blocks. *Nature* **2020**, *583*, 400–405.
(77) Das, A.; Maity, B.; Koley, D.; Ghosh, S. Slothful gelation of a dipolar building block by "top-down" morphology transition from microparticles to nanofibers. *Chem. Commun.* **2013**, *49*, 5757–5759.
(78) Fukui, T.; Kawai, S.; Fujinuma, S.; Matsushita, Y.; Yasuda, T.; Sakurai, T.; Seki, S.; Takeuchi, M.; Sugiyasu, K. Control over differentiation of a metastable supramolecular assembly in one and two dimensions. *Nat. Chem.* **2017**, *9*, 493–499.
(79) Matsumoto, N. M.; Lafleur, R. P. M.; Lou, X.; Shih, K. C.; Wijnands, S. P. W.; Guibert, C.; Van Rosendaal, J. W. A. M.; Voets, I. K.; Palmans, A. R. A.; Lin, Y.; Meijer, E. W. Polymorphism in Benzene-1,3,5-tricarboxamide Supramolecular Assemblies in Water: A Subtle Trade-off between Structure and Dynamics. *J. Am. Chem. Soc.* **2018**, *140*, 13308–13316.
(80) Matern, J.; Dorca, Y.; Sanchez, L.; Fernandez, G. Revising Complex Supramolecular Polymerization under Kinetic and Thermodynamic Control. *Angew. Chem. Int. Ed.* **2019**, *58*, 16730–16740.
(81) Wehner, M.; Röhr, M. I. S.; Bühler, M.; Stepanenko, V.; Wagner, W.; Würthner, F. Supramolecular Polymorphism in One-Dimensional Self-Assembly by Kinetic Pathway Control. *J. Am. Chem. Soc.* **2019**, *141*, 6092–6107.
(82) Greciano, E. E.; Calbo, J.; Ortí, E.; Sánchez, L.; N-Annulated Perylene Bisimides to Bias the Differentiation of Metastable Supramolecular Assemblies into J- and H-Aggregates. *Angew. Chem. Int. Ed.* **2020**, *59*, 17517–17524.
(83) Isobe, A.; Prabhu, D. D.; Datta, S.; Aizawa, T.; Yagai, S. Effect of an Aromatic Solvent on Hydrogen-Bond-Directed Supramolecular

Polymerization Leading to Distinct Topologies. *Chem. Eur. J.* **2020**, *26*, 8997–9004.
(84) Ten Eikelder, H. M. M.; Markvoort, A. J.; de Greef, T. F. A.; Hilbers, P. A. J. An Equilibrium Model for Chiral Amplification in Supramolecular Polymers. *J. Phys. Chem. B* **2012**, *116*, 5291–5301.
(85) Aratsu, K.; Shimizu, N.; Takagi, H.; Haruki, R.; Adachi, S.; Yagai, S. Effect of Solvent on the Thermodynamic Stability of Toroidal Supramolecular Polymers. *Chem. Lett.* **2020**, *49*, 178–181.
(86) Yagai, S.; Ohta, K.; Gushiken, M.; Iwai, K.; Asano, A.; Seki, S.; Kikkawa, Y.; Morimoto, M.; Kitamura, A.; Karatsu, T. Photoreversible Supramolecular Polymerisation and Hierarchical Organization of Hydrogen-Bonded Supramolecular Co-polymers Composed of Diarylethenes and Oligothiophenes. *Chem. Eur. J.* **2012**, *18*, 2244–2253.
(87) Langenstroer, A.; Kartha, K. K.; Dorca, Y.; Droste, J.; Stepanenko, V.; Albuquerque, R. Q.; Hansen M. R.; Sánchez, L.; Fernández, G. Unraveling Concomitant Packing Polymorphism in Metallosupramolecular Polymers, *J. Am. Chem. Soc.* **2019**, *141*, 5192–5200.
(88) Wehner, M.; Röhr, M. I. S.; Stepanenko, V.; Würthner, F. Control of self-assembly pathways toward conglomerate and racemic supramolecular polymers. *Nat. Commun.* **2020**, *11*, 5460.
(89) Matern, J.; Kartha, K. K.; Sánchez, L.; Fernández, G. Consequences of hidden kinetic pathways on supramolecular polymerization. *Chem. Sci.* **2020**, *11*, 6780–6788.
(90) Korevaar, P. A.; Newcomb, C. J.; Meijer, E. W.; Stupp, S. I. Pathway Selection in Peptide Amphiphile Assembly. *J. Am. Chem. Soc.* **2014**, *136*, 8540–8543.

Table of Contents artwork